

3D reconstruction of a femoral shape using a parametric model and two 2D fluoroscopic images

Ryo Kurazume, Kaori Nakamura Toshiyuki Okada, Yoshinobu Sato, Nobuhiko Sugano,
Tsuyoshi Koyama, Yumi Iwashita, and Tsutomu Hasegawa

Abstract—In medical diagnostic imaging, an X-ray CT scanner or a MRI system have been widely used to examine 3D shapes or internal structures of living organisms or bones. However, these apparatuses are generally very expensive and of large size. A prior arrangement is also required before an examination, and thus, it is not suitable for an urgent fracture diagnosis in emergency treatment. This paper proposes a method to estimate a patient-specific 3D shape of a femur from only two fluoroscopic images using a parametric femoral model. Firstly, we develop a parametric femoral model by statistical analysis of a number of 3D femoral shapes created from CT images of 51 patients. Then, the pose and shape parameters of the parametric model are estimated from two 2D fluoroscopic images using a distance map constructed by the Level Set Method. Experiments using synthesized images and fluoroscopic images of a phantom femur are successfully carried out and the usefulness of the proposed method is verified.

I. INTRODUCTION

In medical diagnostic imaging, an X-ray CT (Computed Tomography) scanner or a MRI (Magnetic Resonance Imaging) system have been popular apparatuses to examine 3D shapes or internal structures of living organisms or bones. However, these apparatuses are generally very expensive and of large size, and thus, they are usually installed in large medical institutions rather than small clinics in town. A prior arrangement is also required before an examination, and thus, it is not suitable for an urgent fracture diagnosis in emergency treatment.

On the other hand, X-ray/fluoroscopy has been widely used as traditional medical diagnosis. Recently digital fluoroscopy has been developed and widely used in many hospitals. The cost of this fluoroscopic inspection system is much lower than CT or MRI systems and the system can be dealt with more conveniently. Furthermore, the risk of radiation exposure is also lower than the CT inspection system.

From the above consideration, if it can realize to reconstruct precise 3D shapes of living organisms or bones from few conventional 2D fluoroscopic images, it might be very useful in practice in views of cost, labor, and

radiation exposure. Especially, there is a strong demand from surgeons that 3D computer aided surgery without laborious CT imaging should be offered for some simple surgeries such as artificial joint replacement or fracture treatment. They have desired a 3D diagnostic system using favorite 2D fluoroscopic images.

However, 3D shape reconstruction from a 2D image is a fundamentally ill-posed problem, and thus a plenty of images must be given or some constraint conditions for the 3D shape must be determined. But the shapes of bones have their inherent and universal patterns, and thus by modeling such inherent patterns, 3D shape reconstruction from few 2D images becomes possible.

This paper presents a method to estimate a patient-specific 3D shape of a femur from only two fluoroscopic images. This technique utilizes a parametric femoral model constructed by statistical analysis of a number of 3D femoral shapes created from by CT images of 51 patients. Then, the pose and shape parameters of the parametric model are estimated from two 2D fluoroscopic images using a distance map constructed by the Level Set Method. Experiments using synthesized images and fluoroscopic images of a phantom femur are successfully carried out and the usefulness of the proposed method is verified.

II. RELATED WORKS

2D/3D registration problem is well established in image processing, especially for texture mapping in Computer Graphics or Augmented Reality. For a rigid object, 1) feature-based technique [1],[2],[3], 2) image-based technique using 3D texture, reflectance, brightness, and shading [4],[5],[6], 3) silhouette-based technique [7],[8],[9],[10], have been proposed so far. Especially in surgical navigation system, DRRs (Digitally Reconstructed Radiographs) [22],[23] are widely used in 2D/3D registration for the fluoroscopy-guided surgery.

On the other hand, in 2D/3D registration of a non-rigid object such as soft tissues in medical imaging, similarity measure [11], affine [12], geometric hashing [13], quadric/superquadric [14], and displacement-field-based transformation [15] have been proposed and tested. In addition, the 3D shape estimation of a parameterized object has also been studied such as the shape reconstruction of mathematical plaster models with unknown parameters using a laser range finder [16], or the comparison of multiple cross-section images of a 3D model and a 3D parametric model [17]. However, these studies assumes the use of a plenty of

R. Kurazume and T. Hasegawa are with Graduate Faculty of Information Science and Electrical Engineering, Kyushu University, 744 Motoooka, Nishiku, Fukuoka, Japan kurazume@is.kyushu-u.ac.jp

K. Nakamura and Y. Iwashita is with Graduate School of Information Science and Electrical Engineering, Kyushu University, 744 Motoooka, Nishiku, Fukuoka, 819-0395, Japan

T. Okada is with Graduate School of Information Science and Technology, Osaka University, 1-3, Machikaneyama-cho, Toyonaka-shi, 560-8531, Japan

Y. Sato, N. Sugano, and T. Koyama are with Graduate School of Medicine, Osaka University, 2-2 Yamadaoka, Suita-shi, 565-0871, Japan

	Features	Region
V_{Hc}	Point	center of femoral head
A_P	Line	principal axis of femur
A_N	Line	femoral neck axis
P_{Nc}	Surface	cross section of neck center
V_{Gt}	Surface	apex of greater trochanter
V_{Lt}	Point	lesser trochanter
V_{LP}	Point	iliofemoral ligament attachment
L_R	Curve	ridgeline of greater trochanter
L_V	Curve	valley of greater trochanter

TABLE I
LIST OF ANATOMICAL FEATURES OF FEMUR

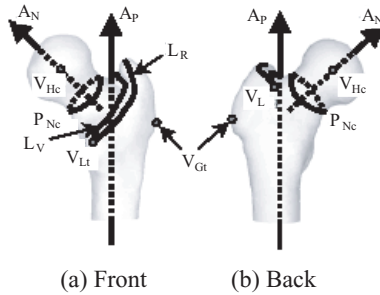


Fig. 1. Anatomical features of femur

images or a precise 3D shape taken by a laser range finder, and only a few studies of 3D non-rigid shape reconstruction from only two or few 2D images have been proposed so far [29],[27],[28].

III. 3D PARAMETRIC FEMORAL MODEL

A. Construction of parametric femoral model

We utilize a statistical shape model of a femur proposed by Okada [18]. In this technique, a number of 3D femoral shapes created from CT images is analyzed statistically, and the parametric femoral model [19] which consists of an average 3D shape and several shape parameters is created. With this parametric femoral model, a general 3D shape of a femur is expressed with the average shape and batch of shape parameters.

The concrete procedure for creating a parametric 3D femoral model is as follows:

1. Anatomical features of a femur are determined automatically or by hand as shown in Table I and Fig. 1.
2. According to the extracted anatomical features, the femur is divided by 4 regions (femoral head, femoral neck, greater trochanter, and femoral shaft). Spherical and cylindrical coordinate systems are defined in each region.
3. In each coordinate system, intersection points of lines which distribute uniformly in the coordinate system and the bone surface are defined as the surface points. 3D coordinates of the surface points are extracted and unique labels are assigned.
4. Steps 1 to 3 are repeated for a plenty number of samples and an average shape is calculated. Next, for each sample, the surface points with

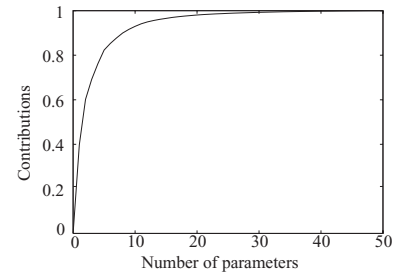


Fig. 2. Contributions of parametric model

same labels are compared with the average shape and displacement vectors are calculated. Then, the principal component analysis (PCA) is applied to the matrix consisting of displacement vectors and several shape parameters are extracted as principal components and vectors.

The parametric femoral model used in the following experiments was created using CT images of 51 patients. By applying PCA to 51 samples of 3D femoral shapes, we extracted the most significant 50 principal components (p_1, p_2, \dots, p_{50}), standard deviation ($\sigma_1, \sigma_2, \dots, \sigma_{50}$), and corresponding principal vectors (v_1, v_2, \dots, v_{50}). With the obtained parametric femoral model, the general 3D shape of a femur is expressed as

$$x' = x + (p_1 \cdot \sigma_1 \cdot v_1) + (p_2 \cdot \sigma_2 \cdot v_2) + \dots \quad (1)$$

where x is the surface point of the average shape and x' is the surface point of the general shape. Therefore, the general 3D shape of a femur is expressed by the parametric femoral model with

- average 3D shape and several principal vectors (pre-determined)
- several (up to 50) shape parameters (estimated)

Figure 2 shows the contribution ratio of the shape parameters for the statistical femoral model.

IV. RECONSTRUCTION OF 3D FEMORAL SHAPE FROM TWO 2D FLUOROSCOPIC IMAGES

In this section, we introduce the 2D/3D registration algorithm and the estimation procedure of the optimum shape parameters using two fluoroscopic images.

This 2D/3D registration algorithm utilizes the contour lines of the silhouette of the 2D image and the projected contour lines of the 3D model. The optimum pose of the 3D model is determined so that both contour lines coincide each other on the 2D image plane. In popular approaches such as ICP algorithm, the error metric is usually defined as the sum of the distances between the points on the 2D contour lines and their nearest points on the projected contour lines of the 3D model. However, the nearest point search is a laborious task and time consuming even for the kd tree-based algorithm [25].

In our approach, the 2D distance map [7] is utilized. Firstly, the 2D distance map from the contour lines is created on the 2D image using the Fast Marching Method [21] or

raster scan algorithms [24]. Once the 2D distance map is created, the error metric is obtained directly from the 2D distance map as a value at the points on the projected contour lines of the 3D model. By taking the course to fine strategy named the “Distance Band” [7], the 2D distance map can be constructed quite rapidly using the Fast Marching Method.

In case that 2D/3D registration and estimation of the shape parameters are performed at the same time, the depth from the view point and the scale of the 3D model cannot be distinguished. Therefore, the proposed algorithm utilizes two fluoroscopic images taken from two viewpoints at different positions. In addition, we assume that the 3D femoral parametric model is constituted by a large number of small triangle patches with almost same size.

A. Registration of 2D fluoroscopic images and 3D parametric model

The brief registration procedure of the 2D fluoroscopic images and the 3D parametric model is as follows:

1. Extract contour lines of the femur in the fluoroscopic images using active contour model such as snakes or Level Set Method [20].
2. Construct 2D distance map from the extracted contour lines using the Fast Marching Method [21]. Figure 3 shows an example of the constructed 2D distance map of a femoral image.
3. Place the parametric femoral model at an arbitrary position and calculate the 2D projection image of the 3D model.
4. Extract contour lines of the projected image and corresponding 3D patches of the 3D model. This procedure can be executed by the OpenGL hardware accelerator quite rapidly.
- 5(a). Apply the force which is calculated from the 2D distance map at the projected contour points directly to the corresponding 3D patch. Details are shown in the following section D.
- 6(a). Using the robust M-estimator, which is one of the robust estimation techniques, the total force and moment around the center of gravity is calculated.
- 7(a). The above procedure from steps 3 to 6(a) is repeated for all the images taken from the different view points and the total force and moment are calculated.
- 8(a). Update the pose of the 3D parametric model according to the total force and moment.
- 9(a). Repeat from steps 3 to 7(a) until the magnitude of the total force and moment becomes less than the pre-defined threshold value.

B. Estimation of the shape parameters

Estimation procedure of the optimum shape parameters of the 3D parametric femoral model is shown in this section. This procedure also uses the 2D distance map from the contour line of the femur in the fluoroscopic image, which has already been constructed as the above section.

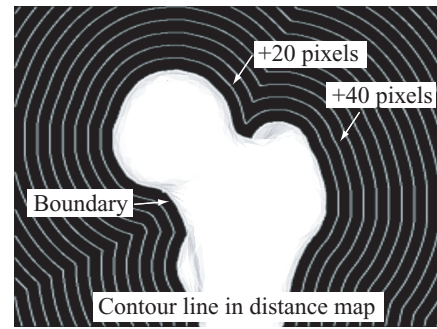


Fig. 3. 2D distance map for femoral image

After step 4 of the above procedure, optimum shape parameters are estimated as follows:

- 5(b). Calculate the error E which is defined as the sum of the value of the 2D distance map at the projected contour line of the 3D parametric model.
- 6(b). Find the optimum shape parameters which minimizes the error E at the current pose using the conjugate gradient method.
- 7(b). Reconstruct the 3D shape according the obtained shape parameters using Eq.(1).
- 8(b). Repeat from steps 3 to Step 7(b) until the error E becomes less than the pre-defined threshold value.

C. Fast extraction of the projected contour line of the 3D parametric femoral model

The contour detection and identifying triangular patches on the 3D model corresponding to points on the contour line are computationally expensive and time consuming. In our implementation, we utilize the high-speed rendering function of the OpenGL hardware accelerator and thus these procedures are executed quite rapidly.

The detailed algorithm is as follows: Initially, we assign different colors for all the triangular patches in the 3D model and draw the projected image of the 3D model on the image buffer using the OpenGL hardware accelerator. The contour points of the 3D model are detected by raster scanning of the image buffer. By reading colors of the detected contour points, we can identify the corresponding triangular patches on the 3D geometric model.

D. 2D/3D registration using the robust M-estimator

After obtaining the distance map on the 2D fluoroscopic image and the list of the triangular patches of the 3D model corresponding to the contour points, the force f_i is applied to all the triangular patches of the contour points (Figs.4 and 5) as explained in Step 5(a).

$$f_i = D_i \frac{\nabla D_i}{|\nabla D_i|} \quad (2)$$

where D_i is the value of the distance map at the contour point, which corresponds to the triangular patch i , and ∇D_i is the gradient of D_i .

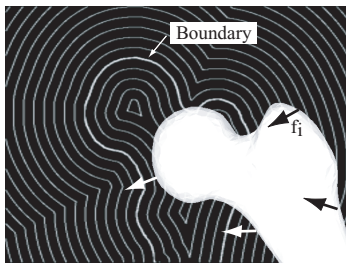


Fig. 4. Force f_i is applied to 3D triangular patch i on contour line

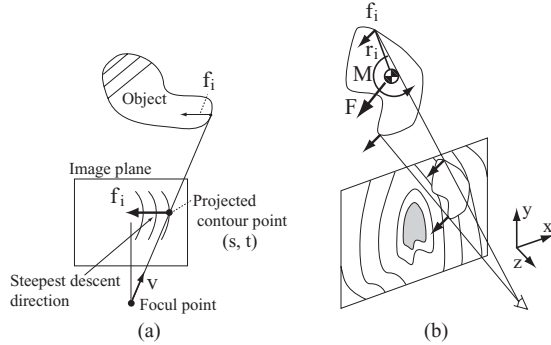


Fig. 5. Total force and moment around center of gravity

In step 6(a), the total force and moment around the center of gravity is calculated with the following equations.

$$F = \sum_i \psi(f_i) \quad (3)$$

$$M = \sum_i \psi(r_i \times f_i) \quad (4)$$

where r_i is a vector from the COG to the triangular patch i and $\psi(z)$ is a particular estimate function. In practical scenario, the contour of the femur is occasionally occluded or blurred, or the 2D image is corrupted by noise. In these cases, the obtained boundary does not coincide with the projected contour of the 3D model and the correct distance value cannot be obtained. To deal with this problem, we introduces the robust M-estimator to ignore contour points with a large amount of errors.

Let's consider the force f_i and the moment $r_i \times f_i$ as an error z_i and the sum of the error as

$$E(P) = \sum_i \rho(z_i) \quad (5)$$

where P is the pose of the 3D parametric model and $\rho(z)$ is a particular estimate function which is defined as

$$\frac{\partial \rho(z)}{\partial z} = \psi(z) \quad (6)$$

The pose P which minimizes the error $E(P)$ is obtained as the following equation.

$$\frac{\partial E}{\partial P} = \sum_i \frac{\partial \rho(z_i)}{\partial z_i} \frac{\partial z_i}{\partial P} = 0 \quad (7)$$

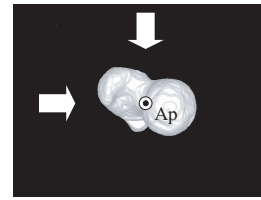


Fig. 6. Directions of fluoroscopic images

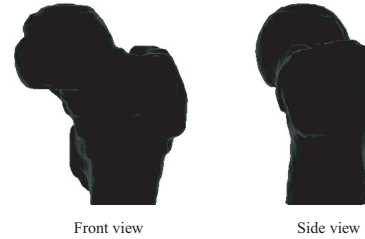


Fig. 7. Reconstructed fluoroscopic images

Here, we define the weight function $w(z)$ as the following equation in order to evaluate the error term.

$$w(z) = \frac{1}{z} \psi(z) = \frac{1}{z} \frac{\partial \rho(z)}{\partial z} \quad (8)$$

From the above equation, we obtain the following weighted least squares method.

$$\frac{\partial E}{\partial P} = \sum_i w(z_i) z_i \frac{\partial z_i}{\partial P} = 0 \quad (9)$$

In our implementation, the optimum pose which minimizes the error $E(P)$ is obtained by the steepest gradient method as shown in step 9(a).

V. EXPERIMENTS

A. Simulation using DRRs

Firstly we conducted the experiments using DRRs (Digitally Reconstructed Radiographs) to evaluate the fundamental performance of the proposed method. In the experiment, the estimation accuracy for 10 femoral models is examined using two reconstructed fluoroscopic images. Among 10 models, 5 models (modeldata1 ~ 5) are used for the construction of the 3D parametric model and 5 models (testdata1 ~ 5) are not used.

We determine the directions of the fluoroscopic images as shown in Fig.6 considering the possible direction in actual radiographic examination. In this condition, two view directions meet at right angles at the main axis of the femur A_P . Examples of the reconstructed fluoroscopic images are shown in Fig.7.

All of the 3D femoral shape used in the experiments were reconstructed precisely by the CT scanner beforehand, and the optimized shape parameters which minimizes distance errors between surface points were determined by comparing the 3D actual shape and the 3D parametric model and searching all possible candidates (ground truth).

Firstly, we chose up to 10 principle components and estimated the pose and the optimum shape parameters of

the femur on the fluoroscopic images. In this experiment, the pose estimation of the femur and the optimum parameter estimation were repeated alternatively and independently. An example of the experimental results for testdata 4 is shown in Fig.8 which illustrates the average shape, the actual shape and the estimated shape, respectively.

Figure 9 indicates the average error between the estimated shape and the actual shape. The average error is defined as the average of the minimum distance from the surface point of the estimated shape to the triangle patches of the actual shape. In this figure, “A” on the horizontal axis indicates the average error at the initial pose and initial shape parameters (all the parameters are set to “0”) before registration, and “0” indicates the average error when the pose is estimated but all the shape parameters are fixed to initial values. This figure shows that the average error gradually decreases as the number of the estimated shape parameters increases. However, the average error converges when the number of the shape parameters is around 5 and no significant difference is observed even if the number of the shape parameters increases.

In addition, Fig.10 shows kinds of errors defined as follows in case that the number of the estimated shape parameters is 5. Figure II also indicates the average of the error, the standard deviation, maximum value, and minimum value for 10 models.

Average error 1

The average error between the average model and the actual shape at the initial pose

Average error 2

The average error between the 3D optimized estimated shape and the 3D actual shape by comparing the actual shape and the parametric model (ground truth).

Average error 3

The average error between the estimated shape and the actual shape by comparing the two 2D fluoroscopic images and the 3D parametric model (proposed method).

The experimental results show that the average error 3 between the estimated shape and the actual shape is less than 1.1 mm at worst and it is verified that the 3D shape can be estimated using the two 2D fluoroscopic images with the same accuracy in case that the 3D shapes are compared directly. Moreover, it is confirmed that there is no significant difference between models which are used for the construction of the parametric femoral model and not used.

B. Experiments using phantom femur

We conducted the experiments using a dry bone of a femur and fluoroscopic images. In the experiments, the special fluoroscopic imaging apparatus (Siemens, Siremobil ISO-C) was used for the fluoroscopic photography from various directions around the phantom femur.

Firstly, we captured images of calibration markers with 9 glass bubbles (left of Fig.11) at 50 positions around

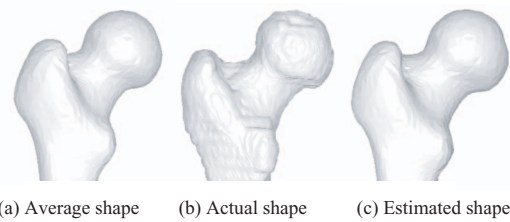


Fig. 8. Femoral model used for shape parameter estimation

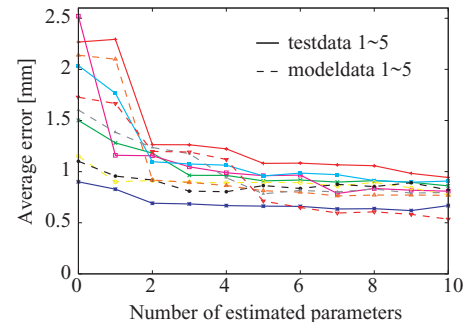


Fig. 9. Average error for numbers of estimated shape parameters

the markers from 0 to 190 degrees using the fluoroscopic apparatus. 3D positions of the markers were also measured by the CT scanner precisely. Next, the intrinsic and extrinsic parameters of the fluoroscopic apparatus were calibrated by the Tsai's method [26].

After the calibration, we replaced the markers with the dry bone of a femur and captured 50 images at the same positions. In addition, the precise 3D shape of the dry bone was measured by the CT scanner. Next, we chose two fluoroscopic images from 50 images as mentioned below and estimated the pose and the optimum parameters in fluoroscopic images using the propose techniques. The examples of the fluoroscopic images are shown in Fig.12.

Figure 13 shows one example of the pair (No.4 and 24) of the fluoroscopic images, which were captured from the directions crossing at right angles. The average errors of the estimated femoral shape are shown in Fig.14 and Table III for the various number of shape parameters used for the estimation. The estimation process and the estimated 3D shape in case that the number of the estimated shape parameters is 10 are shown in Figs.15 and 16. The calculation time is about 1 minute by Pentium IV, 3.2GHz, which includes the contour detection by the Level Set Method and the shape parameter estimation.

Finally, the average errors for various pairs of the fluoroscopic images are shown in Fig.17 in case that the number of the estimated shape parameters is 10. As the results of a series of experiments using the phantom femur, we concluded that the 3D shape can be estimated with the average error of less than 1.2 mm if we choose the proper images captured from the directions crossing at about right angles.

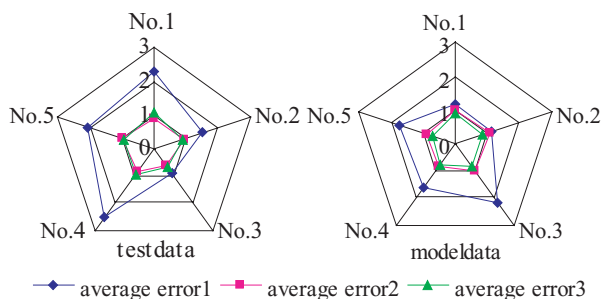


Fig. 10. Average error after shape parameter estimation (number of principle component is 5)

	average	STD.	maximum	minimum
Average error 1	1.69	0.54	2.52	0.90
Average error 2	0.90	0.13	1.06	0.60
Average error 3				
(testdata)	0.91	0.15	1.08	0.66
(modeldata)	0.81	0.07	0.90	0.71

TABLE II
COMPARISON OF AVERAGE ERRORS (MM)

VI. CONCLUSIONS

We proposed a method to estimate a 3D shape of patient's femur from only two fluoroscopic images using a parametric femoral model. Though a precise 3D shape of a femur is usually measured by a CT scanner or a MRI system, our method enables to estimate a precise 3D shape with only two fluoroscopic images taken by a low cost fluoroscopic inspection apparatus. Thus the cost of the inspection system can be dramatically reduced and the 3D image-based medical diagnosis becomes available even in small clinics.

The experimental results show that the average error between the estimated shape and the actual shape is less than 1.1 mm at worst, and it is verified that the 3D shape can be estimated using the two 2D fluoroscopic images taken from the different view points with the same accuracy in case that the 3D shapes are compared directly.

Our future works includes study of the optimum conditions such as the optimum number and directions of the fluoroscopic images, and clinical experiments in fluoroscopic image diagnosis.

REFERENCES

- [1] I. Stamos and P. K. Allen. Integration of range and image sensing for photorealistic 3d modeling. In *Proc. of the 2000 IEEE International Conference on Robotics and Automation*, pp. 1435–1440, 2000.
- [2] I. Stamos and P. K. Allen. Automatic registration of 2-d with 3-d imagery in urban environments. In *Proc. of the International Conference on Computer Vision*, pp. 731–737, 2001.
- [3] L. Liu and I. Stamos. Automatic 3d to 2d registration for the photorealistic rendering of urban scenes. In *IEEE International Conference on Robotics & Automation*, 2005.
- [4] R. Kurazume, K. Noshino, Z. Zhang, and K. Ikeuchi. Simultaneous 2d images and 3d geometric model registration for texture mapping utilizing reflectance attribute. In *Proc. of Fifth Asian Conference on Computer Vision (ACCV)*, pp. 99–106, 2002.
- [5] M. D. Elstrom and P. W. Smith. Stereo-based registration of multi-sensor imagery for enhanced visualization of remote environments. In *Proc. of the 1999 IEEE International Conference on Robotics and Automation*, pp. 1948–1953, 1999.

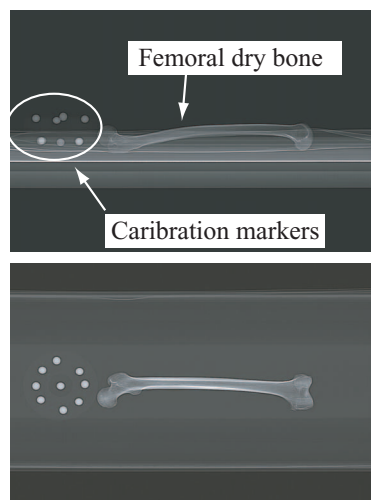


Fig. 11. Fluoroscopic images of calibration markers and phantom femur

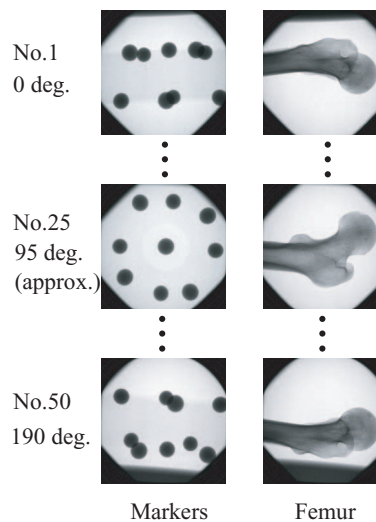


Fig. 12. Measured fluoroscopic images

- [6] K. Umeda, G. Godin, and M. Rioux. Registration of range and color images using gradient constraints and range intensity images. In *Proc. of 17th International Conference on Pattern Recognition*, pp. 12–15, 2004.
- [7] Y. Iwashita, R. Kurazume, K. Hara, and T. Hasegawa. Fast Alignment of 3D Geometrical Models and 2D Color Images using 2D Distance Maps, in *Proc. The 5th International Conference on 3-D Digital Imaging and Modeling (3DIM)*, pp.164-171, 2005.
- [8] Q. Delamarre and O. Faugeras. 3d articulated models and multi-view tracking with silhouettes. In *Proc. of the International Conference on Computer Vision*, Vol. 2, pp. 716–721, 1999.
- [9] K. Matsushita and T. Kaneko. Efficient and handy texture mapping on 3d surfaces. In *Comput. Graphics Forum 18*, pp. 349–358, 1999.
- [10] P. J. Neugebauer and K. Klein. Texturing 3d models of real world objects from multiple unregistered photographic views. In *Computer Graphics Forum 18*, pp. 245–256, 1999.
- [11] C. V. Stewart, C. L. Tsai, and A. Perera. A view-based approach to registration: Theory and application to vascular image registraion. In *International Conference on Information Processing in Medical Imaging (IPMI)*, pp. 475–486, 2003.
- [12] C. V. Stewart, C. L. Tsai, and A. Perera. Rigid and affine registration of smooth surfaces using differential properties. *Proc. of Third European Conference on Computer Vision (ECCV94)*, pp. 397–406, 1994.
- [13] A. Guezic, X. Pennec, and N. Ayache. Medical image registration using geometric hashing. *IEEE Computational Science and Engineering, special issue on Geometric Hashing*, Vol. 4, No. 4, pp. 29–41,

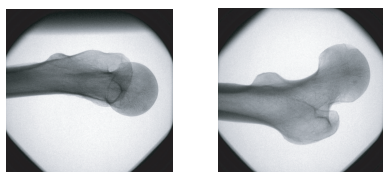


Fig. 13. Fluoroscopic images (No.4 and No.24)

Number of parameters	average	STD.	max.	min.
0	1.973	1.497	7.269	0.0025
1	1.943	1.431	6.801	0.0001
2	1.460	1.153	5.151	0.0011
3	1.039	0.865	3.973	0.0010
4	1.085	0.936	4.476	0.0007
5	1.024	0.886	4.316	0.0013
6	1.017	0.866	4.130	0.0010
7	0.989	0.807	3.980	0.0010
8	0.984	0.784	3.963	0.0010
9	1.041	0.838	4.240	0.0003
10	0.992	0.812	3.952	0.0013

TABLE III

AVERAGE OF ESTIMATION ERRORS OF PHANTOM FEMUR [MM]

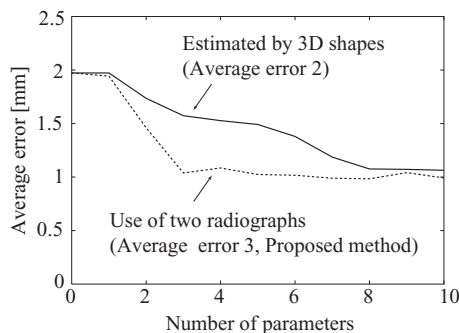


Fig. 14. Estimation errors for numbers of parameters

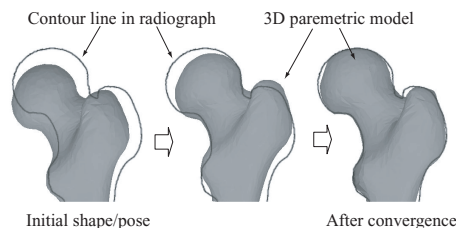


Fig. 15. Process of shape and pose estimation

1997.

[14] Eric Bardinet, Laurent D. Cohen, and Nicholas Ayache. A parametric deformable model to fit unstructured 3d data. *Computer Vision and Image Understanding*, Vol. 71, No. 1, pp. 39–54, 1998.

[15] P. R. Andresen and M. Nielsen. Non-rigid registration by geometry constrained diffusion. *Medical Image Computing and Computer-Assisted Intervention(MICCAI' 99)*, pp. 533–543, 1999.

[16] T. Masuda, Y. Hirota, K. Ikeuchi, and K. Nishino. Simultaneous determination of registration and deformation parameters among 3d range images. In *Fifth International Conference on 3-D Digital Imaging and Modeling*, pp. 369–376, 2005.

[17] CSK Chan, DC Barratt, PJ Edwards, GP Penney, M Slomczykowski, TJ Charter, and DJ Hawkes. Cadaver validation of the use of ultrasound for 3d model instantiation of bony anatomy in image guided orthopaedic surgery. In *Lecture Notes in Computer Science, 3217 (Proc. 7th International Conference on Medical Image Computing and Computer Assisted Intervention, Part II (MICCAI 2004), St-Malo, France)*, pp. 397–404, 2004.

[18] T. Okada, M. Nakamoto, Y. Sato, N. Sugano, H. Yoshikawa, S. Tamura, T. Asaka, Y.-W. Chen. Effects of surface correspondence methods in statistical shape modelling of the proximal femur on approximation accuracy In *Proc. of the 20th International Congress and Exhibition, Computer Assisted Radiology and Surgery CARS 2006*, 016, 2006.

[19] TF Cootes TF, CJ Cooper, CJ Taylor, and J Graham. Active shape models — their training and application,. *Computer Vision and Image Understanding*, Vol. 61, No. 1, pp. 38–59, 1995.

[20] J. Sethian. *Level Set Methods and Fast Marching Methods, second edition*. Cambridge University Press, UK, 1999.

[21] J. Sethian. A fast marching level set method for monotonically advancing fronts. In *Proc. of the National Academy of Science*, Vol. 93, pp. 1591–1595, 1996.

[22] G. Penny, J. Weese, J. Little, P. Desmedt, D. Hill, and D. Hawkes. A Comparison of Similarity Measures for Use in 2-D/3-D Medical Image Registration, *IEEE Trans. Medical Imaging*, Vol.17, No.4, pp.586-595, 1998.

[23] L. Zollei, E. Grimson, A. Norbash, and W. Wells, 2D-3D rigid registration of x-ray fluoroscopy and CT images using mutual information and sparsely sampled histogram estimators, In *Proc. of Computer Vision and Pattern Recognition*, pp.696–703, 2001.

[24] S. W. Shih and Y. T. Wu, Fast Euclidean distance transformation in two scans using a 3 3 neighborhood, *Computer Vision and Image Understanding*, Vol.93, No.2, pp.195–205, 2004.

[25] M. Greenspan, M. Yurick, Approximate k-d tree search for efficient ICP, in *Proc. of 3-D Digital Imaging and Modeling (3DIM) 2003* pp.442–448, 2003.

[26] R. Y. Tsai, An Efficient and Accurate Camera Calibration Technique for 3D Machine Vision, in *Proc. of IEEE Conference on Computer Vision and Pattern Recognition*, pp. 364-374, 1986.

[27] K. Nakamura, R. Kurazume, T. Okada, Y. Sato, N. Sugano, and T. Hasegawa, 3D reconstruction of a femoral shape using a parametric model and two 2D radiographs In *Proc. of Meeting on Image Recognition and Understanding*, pp.78-83, 2006.

[28] G. Zheng, M. Ballester, M. Styner, and L. Nolte, Reconstruction of Patient-specific 3D Bone Surface from 2D Calibrated Fluoroscopic Images and Point Distribution Model In *Proc. of Medical Image Computing and Computer-Assisted Intervention(MICCAI'06)*, pp.25-32, 2006.

[29] D. Terzopoulos and D. Metaxas, Dynamic 3D Models with Local and Global Deformations: Deformable Superquadrics, *IEEE Trans. on Pattern Analysis and Machine Intelligence*, Vol 13, No.7, pp.703-714, 1991.

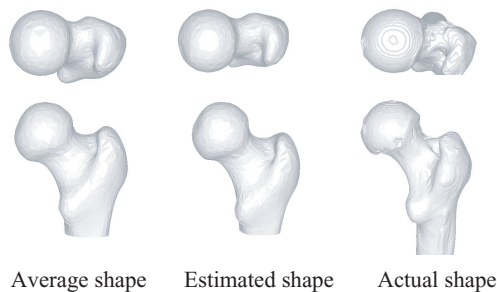


Fig. 16. Estimated shapes of femur

Image No.	[mm]				
	4	14	24	34	44
4 (≈15 deg.)		1.246	0.992	1.128	1.377
14 (≈53 deg.)	-	-	0.980	1.050	1.223
24 (≈91 deg.)	-	-	-	1.143	1.091
34 (≈129 deg.)	-	-	-	-	1.504
44 (≈167 deg.)	-	-	-	-	-

Fig. 17. Estimation errors for various pairs of fluoroscopic images